LETTER

https://doi.org/10.1038/s41586-019-1359-0

Reconstructing the late-accretion history of the Moon

Meng-Hua Zhu[1,2]*, Natalia Artemieva[2,3,4], Alessandro Morbidelli[5], Qing-Zhu Yin[6], Harry Becker[7] & Kai Wünnemann[2,7]

The importance of highly siderophile elements (HSEs; namely, gold, iridium, osmium, palladium, platinum, rhenium, rhodium and ruthenium) in tracking the late accretion stages of planetary formation has long been recognized. However, the precise nature of the Moon's accretional history remains enigmatic. There is a substantial mismatch in the HSE budgets of the Earth and the Moon, with the Earth seeming to have accreted disproportionally more HSEs than the Moon[1]. Several scenarios have been proposed to explain this conundrum, including the delivery of HSEs to the Earth by a few big impactors[1], the accretion of pebble-sized objects on dynamically cold orbits that enhanced the Earth's gravitational focusing factor[2], and the 'sawtooth' impact model, with its much reduced impact flux before about 4.10 billion years ago[3]. However, most of these models assume a high impactor-retention ratio (the fraction of impactor mass retained on the target) for the Moon. Here we perform a series of impact simulations to quantify the impactor-retention ratio, followed by a Monte Carlo procedure considering a monotonically decaying impact flux[4], to compute the impactor mass accreted into the lunar crust and mantle over their histories. We find that the average impactor-retention ratio for the Moon's entire impact history is about three times lower than previously estimated[1,3]. Our results indicate that, to match the HSE budgets of the lunar crust and mantle[5,6], the retention of HSEs should have started 4.35 billion years ago, when most of the lunar magma ocean was solidified[7,8]. Mass accreted before this time must have lost its HSEs to the lunar core, presumably during lunar mantle crystallization[9]. The combination of a low impactor-retention ratio and a late retention of HSEs in the lunar mantle provides a realistic explanation for the apparent deficit of the Moon's late-accreted mass relative to that of the Earth.

The Moon was formed through the accretion of mantle debris from the proto-Earth and an impactor[10,11]; this mantle material was initially deficient in HSEs, because the strong affinity of these elements for metals relative to silicates means that they partition into metal-rich cores rather than silicate-rich mantles. Ensuing differentiation and core formation further depleted HSEs from the early silicate Moon[12,13]. After its formation the Moon underwent a long-term bombardment[3,4], and a substantial amount of exotic materials was delivered to it. The accretion of extralunar materials after the cessation of core formation can be traced through the enrichment of HSEs in the lunar crust and mantle. The late-arriving impactors—with relative HSE abundances similar to those of chondritic meteorites[13]—replenished the lunar mantle HSE content before the crust formed[5,14]. After the thick crust solidified, only larger impactors could penetrate into the mantle. As a consequence, in most cases later impactor materials have been mixed into 'pristine' lunar crust, which was initially characterized by extremely low HSE abundances[6,15]. Estimates from the HSE contents in mantle-derived magmatic rocks suggests that about 1.7×10^{19} kg of material with a chondritic bulk composition accreted in the lunar mantle[5,14], whereas around 0.45×10^{19} to 1.0×10^{19} kg of chondritic material were mixed into the crust[6,16] (see Methods for details). These accreted masses provide strong constraints on the Moon's impact flux[3,9]. However, the timeline and detailed accretionary process are poorly constrained. Intriguingly, the total mass accreted to the Moon (about 2.1×10^{19} to 2.7×10^{19} kg) is about three orders of magnitude lower than that accreted to the Earth, as inferred from the abundance of HSEs in the Earth's mantle (around 2.0×10^{22} kg; ref. [14]). This is in stark contrast with the ratio of about 20 for the mass accreted for the Earth relative to the Moon expected from collisional cross-sections, after gravitational focusing is taken into account[1–3]. Several scenarios have been proposed to explain this imbalance[1–3,17], but its origin is still enigmatic.

Interpretation of the late-accreted masses as constraints on the accretionary process requires a quantitative evaluation of the fraction of the impactor material that is accreted upon impact (hereafter called the impactor-retention ratio, or f). Impactors hitting the Earth are expected to be almost fully accreted owing to the Earth's high gravity (see Methods and refs [1,3,17]). However, how the retention ratio varied for individual impacts on the Moon is unclear[18]. A rough assumption for f of approximately 0.5–0.6 has frequently been used[1,3]. In order to quantitatively investigate the impactor-retention ratio on the Moon, we performed a suite of oblique impact simulations (with impactor diameters, d, of 10–560 km; impact velocities, v, of 10, 15 or 20 km s^{-1}; and impact angles, a, of 20–80° with respect to the lunar surface) on a spherical Moon, using the iSALE-3D shock physics code[19]. We recorded the fractional mass of the impactor that is not ejected or is ejected with a velocity below the Moon's escape velocity (around 2.4 km s^{-1}) and considered these impactor materials to be retained by the Moon (see Methods). Our simulations show a large variation in impactor-retention ratios on the Moon (see Fig. 1). The retention ratio decreases exponentially with increasing impactor-to-target size ratios (x) for impacts with fixed velocities and angles: a high-angle impact delivers a larger fraction of impactor material than a low-angle impact; and large impactors deliver a proportionally lower fraction of material than do small ones (see Methods).

Using these individual impactor-retention ratios, we conducted a Monte Carlo simulation—assuming an impact flux that follows the crater-production function advocated in ref. [4], the prescribed impact velocities of ref. [20] and the isotropic impact angles of ref. [21]—to reproduce the Moon's impact history and to assess the mass accreted into the lunar crust and mantle. In detail, we converted the impactor size–frequency distribution from the crater-production function of the Moon[4] using crater-to-projectile-size scaling laws[22], and then used this information to generate random impactors forming craters up to the observed basin-sized structures (see Methods). Whether the retained impactor material adds to the lunar crust or to the mantle depends on the penetration depth of the impactor relative to the crustal thickness and the fraction of the impactor material that is expelled from the growing crater and deposited on the surface. If the transient crater depth is larger than the average crust thickness of the Moon, then the fraction

[1]State Key Laboratory of Lunar and Planetary Sciences, Macau University of Science and Technology, Taipa, Macau, China. [2]Museum für Naturkunde, Leibniz Institute for Evolution and Biodiversity Science, Berlin, Germany. [3]Planetary Science Institute, Tucson, AZ, USA. [4]Institute of Geosphere Dynamics, RAS, Moscow, Russia. [5]Département Lagrange, University of Nice–Sophia Antipolis, CNRS, Observatoire de la Côte d'Azur, Nice, France. [6]Department of Earth and Planetary Sciences, University of California at Davis, Davis, CA, USA. [7]Institute für Geologische Wissenschaften, Freie Universität Berlin, Berlin, Germany. *e-mail: mhzhu@must.edu.mo

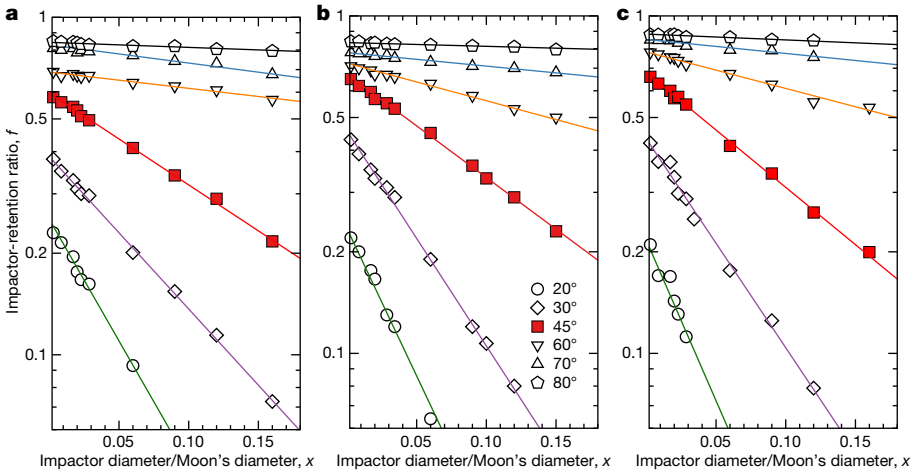

Fig. 1 | Impactor-retention ratios for different velocities, impact angles, and ratios of impactor-to-target sizes. a–c, Simulated impactor-retention ratios (f) for impact velocities of $v = 10$ km s^{-1} (**a**), $v = 15$ km s^{-1} (**b**) and 20 km s^{-1} (**c**), plotted as a function of the ratio of impactor diameter relative to that of the Moon (x). In our simulations, the assigned impact angles (a) were 20°, 30°, 45°, 60°, 70° and 80° relative to the horizontal surface. The points represent the values derived from our iSALE modelling; each line shows a fit with an exponential function of $f = a \times \exp(-b \times x)$. The parameters ($a$, b) of the fitted exponent function are shown in Extended Data Table 1.

of the retained impactor that is emplaced within the transient cavity is considered to deliver its material (and HSEs) to the mantle, while the fraction that is deposited beyond the transient crater is considered to mix with the crust. Otherwise, the retained material is considered to mix with the crust (see Methods). For simplicity, we assume a constant crustal thickness (for example, 34 or 43 km; ref. [23]) from the time of crust formation[24] until the present day. We treated the time at which the mantle and crust started to retain HSEs as a free parameter, and determined the time that allows the simulation to match the observed HSE budgets in the lunar mantle and crust.

We repeated the Monte Carlo procedure millions of times to address the stochastic variability intrinsic in the bombardment process. A key result is that the average impactor-retention ratio for the Moon as a whole depends on the time interval considered (Fig. 2). Early on, more large-size impactors lead to a lower average retention ratio, because large impacts deliver a smaller fraction of impactor material to the Moon (Fig. 1). The average retention ratio integrated over the Moon's impact history since 4.46 billion years (Gyr) ago—the presumed earliest time for the formation of lunar crust[24]—is about 0.20 (Fig. 2), which is about three times lower than the range of 0.5–0.6 that was frequently assumed previously[1,3,9].

For the accreted mass from our simulations to be consistent with that inferred from the HSE concentrations in the lunar mantle, the required time at which the lunar mantle should have begun to retain impactor HSEs is 4.35 Gyr ago—that is, around 150 million years after the presumed lunar formation event[25]. In our model, the mantle has accreted around 1.70×10^{19} kg of impactor material since 4.35 Gyr ago, when the lunar magma ocean (LMO) was mostly solidified and a thick crust was fully formed[26,27] (Fig. 3); about 85% of this mass was typically accreted between 4.35 Gyr and 4.15 Gyr ago. The mantle accreted substantially more material, about 3.0×10^{19} kg, before 4.35 Gyr ago. This suggests that the early mantle of the Moon could have held substantially higher abundances of HSEs than the mantle of the present Moon. Impactor material accreted to the mantle before 4.35 Gyr ago did not leave behind any record in the present HSE budget, either because it was trapped in the deep mantle[5] or because the HSEs partitioned into the core[28] during mantle crystallization and overturn[7,9]. This result supersedes previous assumptions that the HSEs in the lunar mantle accumulated early on, before the formation of a thick crust (see, for example, refs [5,6,14]). Contrary to previous assumptions that late-occurring impacts did not contribute to the HSE budget of the lunar mantle owing to the existence of a thick crust, we find that large impacts can penetrate the thick crust and deliver impactor material into the mantle, even when the crust has been well developed and cooled. However, most of these replenishments by large impacts happened before around 3.85 Gyr ago. After this date, the delivery of impactor material to the mantle has been small (Fig. 3). This is because there are few impacts that can penetrate through the thick lunar crust after this time[29].

If the lunar crust has retained impactor material since 4.46 Gyr ago—its estimated earliest formation time[24]—then the total accreted mass in the lunar crust could be up to around 1.0×10^{19} kg (Fig. 3). For any later retention time, but before 4.35 Gyr ago, the total accreted mass in the crust is within the range of 0.45×10^{19} to 1.0×10^{19} kg inferred from the estimated crustal HSE budget (see, for example,

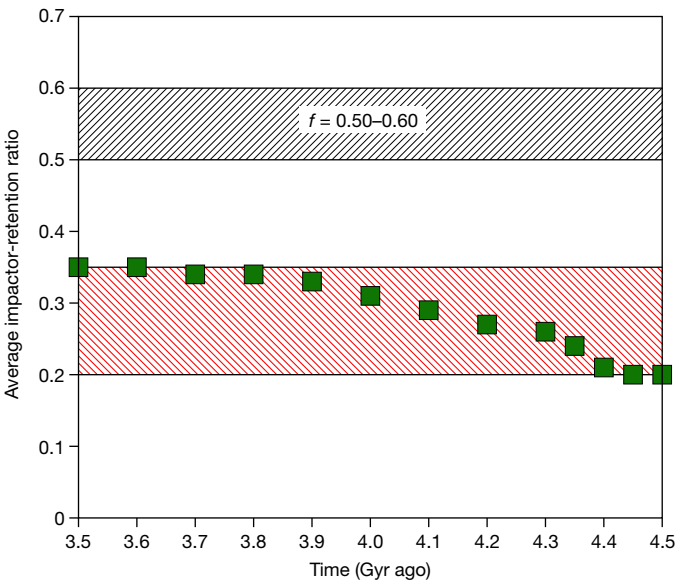

Fig. 2 | Average impactor-retention ratios as a function of time. The Moon's average impactor-retention ratio, f (solid green squares), is defined as the ratio between the total mass accreted to the Moon and the total impactor mass hitting the Moon. For example, the data point at 4.35 Gyr ago represents the average f-value for impacts occurring cumulatively from 4.35 Gyr ago to the present day. In this study, the average f-values are between 0.20 and 0.35 (red hatched area) for a start time between 4.46 Gyr and 3.50 Gyr ago—similar to the range predicted in ref. [2] ($f = 0.16$–0.32) for the entire impact history of the Moon, but about two to three times lower than the values considered in refs [1,3] ($f = 0.50$ or 0.60, the black hatched area, derived from the simulation of small impactors at an oblique angle of 45°; ref. [18]).

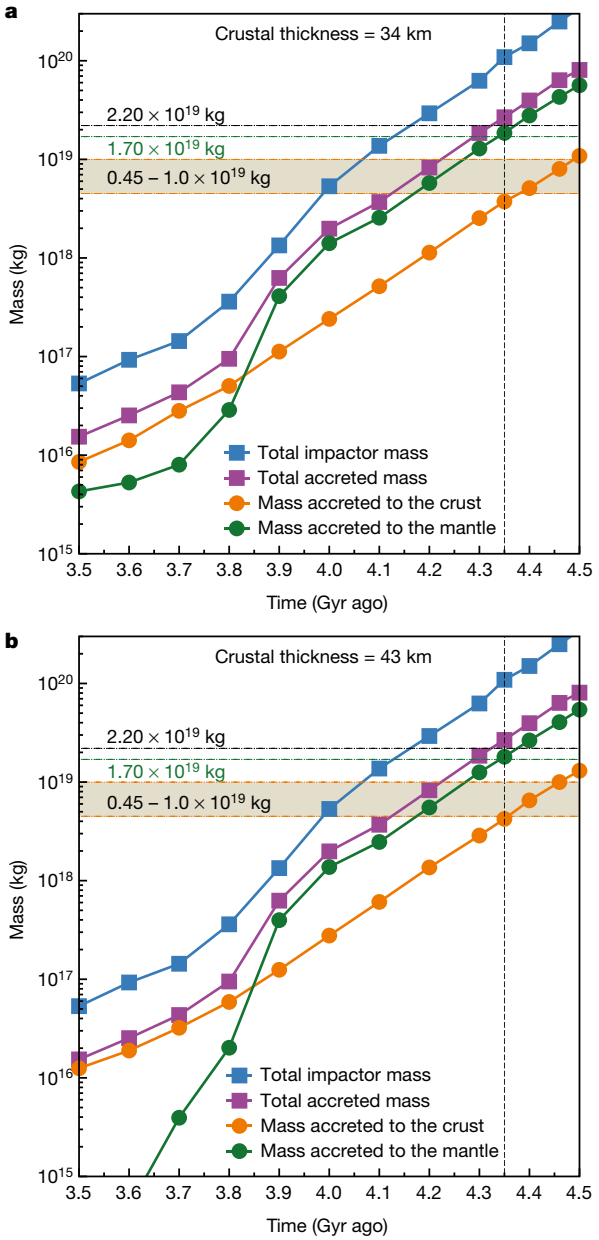

Fig. 3 | Cumulative impactor-mass distribution as a function of time. **a**, **b**, Total impactor masses hitting the Moon (blue) and being accreted onto the Moon (purple) from different starting times (between 4.5 Gyr to 3.5 Gyr ago) to the present day, for assumed crustal thicknesses of 34 km (**a**) and 43 km (**b**). The cumulative masses accreted to the lunar crust (orange) and mantle (green) are estimated separately. Each data point represents the average of millions of Monte Carlo simulations. We assume a projectile density of 3,000 kg m^{-3}. The horizontal black and green dash-dotted lines represent the masses accreted to the silicate part of the Moon (2.20×10^{19} kg) and the mantle (1.70×10^{19} kg) as inferred from HSE budgets[5]; the horizontal orange dash-dotted lines mark the lower (0.45×10^{19} kg) and upper (1.0×10^{19} kg) limits for the mass accreted to the lunar crust, also inferred from HSE budgets[6,16]. The vertical black dotted line marks the time at 4.35 Gyr ago when the masses added to the crust and mantle in the Monte Carlo simulations reach the values (horizontal lines) estimated from the HSEs. The lower (34 km) and upper (43 km) limits for the average crustal thickness used here are based on the observations of GRAIL mission[23]. As lunar crust may have formed (around 4.46 Gyr ago[24]) soon after the Moon's formation[25], for simplicity we assume in our calculations that the global crustal thickness remained constant during lunar history. An evolving crustal thickness, from a few kilometres soon after the Moon's formation to the present thickness at around 4.46 Gyr ago, would not affect the results. In this figure, we assume that around 4% of the retained impactor material is deposited beyond the transient crater and mixed with the crust.

refs [6,16] and Methods). Therefore, this mass range may represent the lower and upper limits of the material accreted to the lunar crust. It indicates that the lunar crustal HSE budget may represent the Moon's accretion history since the crust's earliest formation time (at least since 4.35 Gyr ago, when the LMO was mostly solidified[7,26,27]).

The estimated total mass of impactors hitting the Moon since 4.50 Gyr ago is around 3.7×10^{20} kg (or about $6 \times 10^{-5}\ M_{\oplus}$, where $M_{\oplus}$ is the mass of the Earth; see Fig. 3). This mass is an order of magnitude higher than previous estimates based on the lunar HSE budget ($5 \times 10^{-6}\ M_{\oplus}$; see, for example, ref. [3]), but in agreement with a recent estimate from dynamical considerations[9]. This suggests that the Moon underwent a much more intense early bombardment than previously thought[3]. Our simulations indicate that the impactors should have produced around 300 basins (with diameters of more than 300 km) during the lunar impact history: about 200 basins before 4.35 Gyr ago, 90 basins between 4.35 Gyr and 4.15 Gyr ago, and 20 basins from 4.15 Gyr to the present day. This total is about three to eight times higher than the number of basins (around 40–90) estimated from certain and uncertain structures observed on the lunar surface[30,31]. However, impacts that occurred before 4.35 Gyr ago, during the main phase of LMO crystallization[7], should have failed to produce long-lasting structures because of the low viscosity of the warm crust and mantle. In addition, owing to the viscous relaxation of the target, basins formed just after LMO solidification (around 4.35 Gyr ago) can have existed for about 100 million years at most[32]. Consequently, about 40–50 of the 90 basins that formed between 4.35 Gyr and 4.15 Gyr ago (a period of about 200 million years) were probably erased, whereas the others partially relaxed to some extent. Basins that formed later would have been preserved and remain detectable to the present day. Therefore, according to our model and given basin retention and degradation processes[32], only 50–70 basins in total should be visible, in agreement with the number of basins (about 40–90) observed or inferred on the lunar surface[30,31]. These basins are the only remnants of the heavy bombardment history of the Moon.

Using previous assumptions of an average impactor-retention ratio of 0.5–0.6 (Fig. 2 and refs [1,3]), the impact flux of ref. [4] led to a predicted mass of late-accreted material that was an order of magnitude higher than the mass inferred from the HSEs in the lunar mantle and crust[3]. With our reduced value for the impactor-retention ratio f, the amount of accreted material still exceeds that inferred from the HSE budget, although only by a factor of around three. A sawtooth-like impact flux[3], with a surge in the projectile population at the time of a presumed lunar cataclysm (see Methods), has been proposed to reconcile the impact history of the Moon and the amount of accreted material as inferred from HSEs during the past 4.50 Gyr. However, if the lunar mantle retained HSEs only from 4.35 Gyr ago, then the conceptual sawtooth-like cataclysm scenario[3] is not needed anymore to explain the Moon's impact flux (see Methods).

The good agreement between the time at which the lunar mantle started to retain accreted HSEs (around 4.35 Gyr ago) and the age records from lunar crustal rocks (see, for example, ref. [26]) indicates that the HSE budget of the lunar mantle possibly depends on the time of crystallization of the LMO. Our results support an extended solidification time scale for the LMO of about 150–200 million years after lunar formation[7]. Our results suggest that HSEs accreted during or before LMO crystallization were mostly transported to the lunar core during late-stage metal and sulfide segregation[9].

The estimated total mass of impactors hitting the Moon since 4.50 Gyr ago (roughly 3.7×10^{20} kg) is about a factor of 50 times lower than the mass accreted to the Earth (around 2.0×10^{22} kg; ref. [14]), assuming that the impactors hitting the Earth were fully accreted[1,3,9,17] and retained in the terrestrial mantle owing to the fast crystallization of its magma ocean[33]. The ratio obtained from collisional cross-sections is about 20, implying that the alleged large imbalance in late-accreted mass between the Earth and the Moon[1] no longer exists. The disproportional mass accreted on the Earth and Moon as inferred from HSEs[1,13] is probably a consequence of different impactor-retention ratios,

coupled with different time scales for magma ocean solidification on these bodies.

Online content

Any methods, additional references, Nature Research reporting summaries, source data, extended data, supplementary information, acknowledgements, peer review information; details of author contributions and competing interests; and statements of data and code availability are available at https://doi.org/10.1038/s41586-019-1359-0.

Received: 14 February 2019; Accepted: 23 May 2019;
Published online 10 July 2019.

1. Bottke, W. F. et al. Stochastic late accretion to Earth, the Moon, and Mars. *Science* **330**, 1527–1530 (2010).
2. Schlichting, H. E., Warren, P. H. & Yin, Q.-Z. The last stages of terrestrial planet formation: dynamical friction and the late veneer. *Astrophys. J.* **752**, 8–16 (2012).
3. Morbidelli, A. et al. A sawtooth-like timeline for the first billion years of lunar bombardment. *Earth Planet. Sci. Lett.* **355-356**, 144–151 (2012).
4. Neukum, G., Ivanov, B. A. & Hartmann, W. K. Cratering records in the inner solar system in relation to the lunar reference system. *Space Sci. Rev.* **96**, 55–86 (2001).
5. Day, J. M. D. & Walker, R. J. Highly siderophile element depletion in the Moon. *Earth Planet. Sci. Lett.* **423**, 114–124 (2015).
6. Day, J. M. D. et al. Osmium isotope and highly siderophile element systematics of the lunar crust. *Earth Planet. Sci. Lett.* **289**, 595–605 (2010).
7. Elkins-Tanton, L., Burgess, S. & Yin, Q. Z. The lunar magma ocean: reconciling the solidification process with lunar petrology and geochronology. *Earth Planet. Sci. Lett.* **304**, 326–336 (2011).
8. Borg, L. E. et al. Chronological evidence that the Moon is either young or did not have a global magma ocean. *Nature* **477**, 70–72 (2011).
9. Morbidelli, A. et al. The timeline of the lunar bombardment: revisited. *Icarus* **305**, 262–276 (2018).
10. Canup, R. M. Forming a Moon with an Earth-like composition via a giant impact. *Science* **338**, 1052–1055 (2012).
11. Cuk, M. & Stewart S. T. Making the Moon from a fast-spinning Earth: a giant impact followed by resonant despinning. *Science* **338**, 1047–1052 (2012).
12. Jones, J. H. & Drake, M. J. Core formation and Earth's late accretionary history. *Nature* **323**, 470–471 (1986).
13. Morgan, J. W., Walker, R. J., Brandon, A. D. & Horan, M. F. Siderophile elements in Earth's upper mantle and lunar breccias: data synthesis suggests manifestations of the same late influx. *Meteorit. Planet. Sci.* **36**, 1257–1275 (2001).
14. Walker, R. J. Highly siderophile elements in the Earth, Moon and Mars: update and implications for planetary accretion and differentiation. *Chem. Erde Geochem.* **69**, 101–125 (2009).
15. Warren, P. H., Jerde, E. A. & Kallemeyn, G. W. Prisitine Moon rocks: Apollo 17 anorthosites. *Proc. Lunar Planet. Sci. Conf.* **21**, 51–61 (1991).
16. Ryder, G. Mass flux in the ancient Earth-Moon system and benign implications for the origin of life on Earth. *J. Geophys. Res.* **107** (E4), 5022 (2002).
17. Kraus, R. G. et al. Impact vaporization of planetesimal cores in the late stages of planet formation. *Nat. Geosci.* **8**, 269–272 (2015).
18. Artemieva, N. A. & Shuvalov, V. V. Numerical simulation of high-velocity impact ejecta following falls of comets and asteroids onto the Moon. *Sol. Syst. Res.* **42**, 329–334 (2008).
19. Elbeshausen D. et al. The transition from circular to elliptical impact crater. *J. Geophys. Res.* **118**, 2295–2309 (2013).
20. Le Feuvre, M. & Wieczorek, M. A. Nonuniform cratering of the Moon and a revised crater chronology of the inner solar system. *Icarus* **214**, 1–20 (2011).
21. Shoemaker, E. M. in *Physics and Astronomy of the Moon* (ed. Kopal, Z.) 283–359 (Academic, 1962).
22. Holsapple, K. A. & Housen, K. R. A crater and its ejecta: an interpretation of deep impact. *Icarus* **191**, 586–597 (2007).
23. Wieczorek, M. A. et al. The crust of the Moon as seen by GRAIL. *Science* **339**, 671–675 (2013).
24. Norman, M. D. et al. Chronology, geochemistry, and petrology of a ferroan noritic anorthosite clast from Descartes breccia 67215: clues to the age, origin, structure, and impact history of the lunar crust. *Meteorit. Planet. Sci.* **38**, 645–661 (2003).
25. Kleine, T. et al. Hf-W chronology of the accretion and early evolution of asteroids and terrestrial planets. *Geochim. Cosmochim. Acta* **73**, 5150–5188 (2009).
26. Borg, L. E. et al. A review of lunar chronology revealing a preponderance of 4.34–4.37 Ga ages. *Meteorit. Planet. Sci.* **50**, 715–732 (2015).
27. Nemchin, A. et al. Timing of crystallization of the lunar magma ocean constrained by the oldest ziron. *Nat. Geosci.* **2**, 133–136 (2009).
28. Rubie, D. C. et al. Highly siderophile elements were stripped from Earth's mantle by iron sulfide segregation. *Science* **353**, 1141–1144 (2016).
29. Miljković, K. et al. Excavation of the lunar mantle by basin-forming impact events on the Moon. *Earth Planet. Sci. Lett.* **409**, 243–251 (2015).
30. Neumann, G. A. et al. Lunar impact basins revealed by Gravity Recovery and Interior Laboratory measurements. *Sci. Adv.* **1**, e1500852 (2015).
31. Frey, H. in *Recent Advances and Current Research Issues in Lunar Stratigraphy* Vol. 477 (eds Ambrose, W. A. & Williams, D. A.) 53–75 (Geological Society of America, 2011).
32. Kamata, S. et al. The relative timing of lunar magma ocean solidification and the late heavy bombardment inferred from highly degraded impact basin structures. *Icarus* **250**, 492–503 (2015).
33. Elkins-Tanton, L. Linked magma ocean solidification and atmospheric growth for Earth and Mars. *Earth Planet. Sci. Lett.* **271**, 181–191 (2008).

METHODS

HSE-derived estimates of impactor mass accretion. The masses of impactor material accreted to the crust and mantle of the Moon have been estimated from the concentrations of HSEs in lunar samples (see, for example, refs [5,6,34,35]). The HSE concentrations in the lunar mantle are robustly estimated, regardless of sulfide or metal saturation in the lunar mantle[36]. On the basis of the osmium concentration (about 100 pg g^{-1}) of mantle-derived melts (for example, mare basalts and pyroclastic glasses[5,34,37]) in lunar samples, it is conservatively estimated that about 1.70×10^{19} kg of material with a chondritic bulk composition was added to the lunar mantle[34], assuming that the mass of lunar mantle is about 6.9×10^{22} kg (ref. [38]) and that late-accretion-delivered bodies possess an average osmium concentration of 660 ng g^{-1}, similar to chondrites[14].

For the mass of late-accreted material stored in the crust, estimates based on HSE contents have varied considerably. Day et al.[6] analysed the concentrations of HSEs in the pristine crustal rocks (numbers 60,025, 62,255 and 65,313) from the Moon, and found that the flotation-derived anorthositic crust has a typical osmium concentration of 1.4 pg g^{-1}. By contrast, impact melt breccias and bulk regolith samples contaminated with impactor material have osmium concentrations mostly of 5–15 ng g^{-1} (see refs [39–43]). The extent of contamination of the lunar crust by impactors is uncertain, in particular at greater depths. Estimates range from about 10% of crustal mass (corresponding to the uppermost roughly 5–10 km of crust; see, for example, ref. [6]) to a roughly uniform mixture of impactor material with the crust (see, for example, ref. [2]). With these assumptions, a mass of 0.4×10^{19} kg (ref. [16]), and no more than 14×10^{19} kg (ref. [2]), of material is thought to have been accreted to the lunar crust. However, the high-end estimate of ref. [2] implies a uniform osmium and iridium distribution throughout the lunar crust, which is unrealistic.

The observations of the Gravity Recovery and Interior Laboratory (GRAIL) mission suggest an average crustal thickness of between 34 km and 43 km (ref. [23]). With a bulk density of 2,500 kg m^{-3} (ref. [23]), the mass of the lunar crust is roughly 3.2×10^{21} to 4.1×10^{21} kg. Assuming that the crust has an osmium concentration of between 5 and 15 ng g^{-1}, and that about 10% of the lunar crust was contaminated by impactor material (see, for example, refs [6,37,43]), we recalculated the mass of chondritic material accreted to the lunar crust. Our calculation indicates that chondritic material with a mass of roughly 0.45×10^{19} to 1.0×10^{19} kg was added into the lunar crust, consistent with the early estimates (see, for example, refs [6,16,35]). Here, we use these values as lower and upper limits with which to estimate the time from which substantial masses of impactor material have been retained in the lunar crust.

Impactor-retention ratio on the Moon. In order to investigate the impactor-retention ratio during the bombardment history of the Moon, a detailed quantitative study of the consequences of hypervelocity impacts of cosmic bodies of given mass, velocity and angle of incidence is required. Modelling using shock-physics codes constitutes the most accurate approach by which to estimate the mass of projectiles retained in the crust and mantle as the result of a collision. However, given the large number of collisions on the Moon, it is impossible to model each impact event individually. A parameterization of the relationship between the properties of an impact event (projectile diameter d, impact velocity v, and impact angle a) and the resulting impactor-retention ratio, f, is required. The impactor-retention ratios for individual impacts with different impact angles and relatively low impact velocities (3.0–5.0 km s^{-1}) have been estimated from laboratory impact experiments (for example, refs [44–47]). Whether the results from the terrestrial laboratory experiments can be extrapolated to impactor sizes of several hundreds of kilometres in diameter and to much higher velocities in a low-gravity regime is questionable. Therefore, we have carried out a systematic modelling study to determine the impactor-retention ratio under realistic impact conditions on the Moon, in order to develop parameterizations of the retention ratio as a function of impactor size, angle, and velocity on the Moon.

We use the shock-physics code iSALE-3D (ref. [19]) to conduct a series of three-dimensional numerical models of impacts with projectile diameters d ranging from 10 to 560 km. We approximate the Moon as a 3,500-km-diameter sphere with a 700-km-diameter iron core. The analytic equations of state (ANEOS[48]) for dunite[49] and for iron[48] are used to describe the thermodynamic behaviour of lunar mantle and core, respectively. The initial densities of dunite and iron are assumed to be roughly 3.0 g cm^{-3} and 7.8 g cm^{-3}, respectively. For undifferentiated impactors ($d < 300$ km) we assume a dunitic composition, similar to that of the lunar mantle, whereas for differentiated projectiles ($d > 300$ km) we assume the existence of an iron core that accounts for about 30% of the total mass of the impactor[50]. The present version of iSALE-3D does not allow the consideration of different materials that may mix upon impact. This limitation is not critical for the Moon, because the sizes of the impactors considered here are too small for the projectiles to reach the lunar core–mantle boundary. However, for a differentiated impactor material, mixing of the impactor's core and mantle within the mantle of the Moon obviously occurs. To represent this mixing despite the code limitations, we approximate the differentiated impactor as a homogenous dunitic sphere with a radius a little larger than that of the real one, in order to preserve the total mass. We identify as 'core material' that material within a central sphere with a radius similar to that of the metal core in the differentiated impactor, and then track the fate of this material by tracers. This approximation is plausible because the approximated projectile preserves the size of the metal core and the total mass of the real differentiated impactor; moreover, the size of the impactor does not change substantially. For example, for a differentiated impactor with a radius of 300 km, the metal core has a radius of about 160 km, representing about 30% of the total mass (for example, roughly 4.5×10^{20} kg). For an approximated dunitic sphere of the same mass, the radius is about 319 km. The difference between the radii of the differentiated and approximated impactors is small, and decreases still further for smaller differentiated impactors.

In all models the impactor is resolved by 20 cells per projectile radius (CPPR), which is considered to be sufficient for accurate predictions of the impactor-retention ratio[19,51]. However, for small impactors (for example, $d < 50$ km), this high resolution causes the problem that the entire Moon cannot be modelled with the same resolution, given that the computational domain has a maximum total extent of $700 \times 350 \times 350$ cells. Previous models[52] indicated that the curvature of the Moon does not affect the cratering and ejection process for impactor diameters of less than 50 km. Therefore, for small impactors, we approximate the Moon as a planar target with the same resolution for the impactor (20 CPPR). The high-resolution models are very demanding on computational resources for each simulation. Each simulation lasts for one to two months on a 96-core parallel CPU computer cluster. In total, we ran about 200 oblique-impact models with impact velocities, v, of 10 km s^{-1}, 15 km s^{-1} and 20 km s^{-1}, and impact angles of $a = 20°$, 30°, 45°, 60°, 70° and 80° with respect to the lunar surface. These ranges are considered to represent the most likely impact velocities and angles during the Moon's impact history[20,21,53]. The parameters used in the model are listed in Extended Data Table 2.

Our simulations aim at determining the mass fraction of impactor material deposited on and in the Moon. For each individual impact simulation, we track the impactor material by using Lagrangian tracers in iSALE, which are initially placed in the centre of each computational cell and represent the mass of the original material in the considered cell throughout the simulations (see, for example, ref. [54]). We record the number of impactor tracers that are not ejected or are ejected from the crater with a velocity (v_e) lower than the Moon's escape velocity (2.4 km s^{-1}, and consider that the mass represented by these tracers is retained on the Moon.

Vaporization of the impactor material (that is, dunite) requires a high impact-induced peak shock pressure (of more than about 186 GPa; refs [49,55,56]), and thus high-velocity impacts[57]. Previous work[17,18,57] indicated that the amount of vaporized impactor is limited to a small fraction of the projectile mass for asteroidal impacts with velocities smaller than 20 km s^{-1}, and that the vaporized volume of the impactor decreases with the impact angle relative to the surface. For impacts on the Moon, the average velocity is relatively low, in particular for the early large impacts[58]; therefore, the impactor vaporization has little influence on the impactor-retention ratio for oblique impacts on the Moon[18]. In our simulations, we applied a density cut-off to erase low-density (less than 1 kg m^{-3}) materials that tend to expand at a relatively high velocity, slowing down the computation time substantially. These low-density cells usually represent vaporized impactor and target materials. The fraction of the removed material relative to the total amount of impactor material that is either retained on the Moon or escapes the lunar gravity field is usually negligible. It has been proposed recently that impactor metal cores can vaporize with a shock pressure of about 507 GPa during high-velocity impacts, allowing iron metal to escape from the lunar surface and reducing the accreted mass of impactor material[17]. However, to be effective, this shock pressure requires extremely high impact velocities. For the impact velocities considered here, the amount of vaporized impactor core is very small and therefore can be neglected.

Our simulations indicate that the retention ratio varies greatly with the impact angle (Fig. 1). High-angle impacts lead to a higher retention factor than low-angle impacts, in agreement with the results of the laboratory impact experiments (for example, refs [44–47,59]). This result is not difficult to understand intuitively. For low-angle impacts, most of the impactor is sheared off at high velocity upon impact on the lunar surface, so that such impact scenarios do not add a large amount of impactor mass to the Moon (see also refs [57,59]). For high-angle impacts, most of the impactor material is compacted and forms a veneer lining the crater wall of the transient crater, where it is eventually mixed into the lunar crust or mantle. In addition, for low-angle impacts ($a < 45°$), the cratering efficiency (the ratio of excavated mass to impactor mass) decreases with increasing impactor-to-target-size ratio (x), owing to the dramatically reduced coupling between impactor and target on a curved surface (at a fixed impact angle)[60]. Therefore, material from a large impactor escapes more easily than that from a small one. However, for steep impacts ($a > 45°$), the crater efficiency does not vary greatly with the impactor-to-target-size ratio; as a consequence, the fraction of the impactor accreted on the Moon varies only slightly with the size of impactors at fixed and large impact

angles. Moreover, the impact velocities in our simulations are much larger than the Moon's escape velocity (about 2.4 km s^{-1}). Most ejected impactor material has velocities much higher than the Moon's escape velocity during the course of crater excavation. Thus, impacts with different velocities (at a fixed impact angle) follow qualitatively similar trends regarding the impactor-retention ratio (Fig. 1). Note that, for low-angle impacts, where a substantial amount of impactor material is lost to space, *N*-body simulations have shown that most of the escaped material will re-hit the Earth–Moon system after a few orbits, with a higher (greater than 90%) probability of hitting the Earth[61] rather than the Moon owing to the Earth's larger cross-section. Therefore, we consider that the fraction of the escaped projectile material that subsequently collides with the Moon provides a negligible contribution to the lunar impactor-retention ratio.

In order to derive a simple parameterization of the retention ratio as a function of impactor diameter, impact angle and velocity, we fit the retention fraction from our simulations as a function of impactor-to-target-size ratio (x). We find that the impactor retention ratio decreases while x increases, following an exponential function ($f = a \times \exp(-b \times x)$; here, a and b are the fitted parameters) at fixed impact velocity and angle (Fig. 1). The parameters of the fitted exponential function for the oblique impacts are listed in Extended Data Table 1.

The Moon has experienced a long-term thermal evolution since its formation (see, for example, refs [7,62]). The changing thermal gradient of the Moon has a substantial effect on the formation of large-scale impact basins[63,64]. However, whether the thermal gradient of the Moon affects the impactor-retention ratio is unknown. To quantify this effect, we used two plausible thermal profiles (TP1 and TP2; Extended Data Fig. 1) to represent the general thermal condition of early (warm) and late (cold) Moon. TP1 (cold) has a temperature gradient of 30 K km^{-1} below the lunar surface, and decreases slowly following an adiabatic gradient (0.5 K km^{-1}) from temperatures in excess of 1,300 K (ref. [65]). TP2 (hot) has a temperature gradient of 50 K km^{-1} in the upper 20 km, then follows the solidus of dunite within a depth range of 20–350 km, and remains constant at a temperature of 1,670 K for depths of more than 350 km (ref. [66]). These two temperature profiles are considered to form an envelope of possible thermal conditions of the Moon during its impact history[7,62–67]. The result from our simulations indicates that the impactor-retention ratio is insensitive to the Moon's thermal profile (see Extended Data Fig. 2 for the retention ratios of impactors with $d = 210$ km, $v = 15$ km s^{-1} and impact angles from 15° to 80° on the Moon with the temperature profiles of TP1 and TP2). The temperature and thus the rheology of the target play a minor role during the excavation phase of the crater, when ejection of target and impactor takes place. Subsequently, during the crater modification phase, the thermal state and its softening effect on material strength are much more important; however, at such a late stage of crater formation no further material, and in particular no impactor material, is ejected anymore[68].

We also investigated where the retained impactor material stays on the Moon. For each individual impact, we distinguish two cases for the retained impactor materials: (1) ejected (with ejection velocities of less than 2.4 km s^{-1}, the Moon's escape velocity) but deposited beyond the transient crater on the surface of the Moon; and (2) trapped within the transient crater. According to our simulations, around 90–99% of the retained impactor material remains within the transient crater, and only 1–10% is ejected and deposited beyond the transient crater, depending on the impact angle (see Extended Data Fig. 3 for the percentage of retained impactor located within the transient crater). These values are broadly consistent with the results of laboratory impact experiments, which also show that the vast majority of impactor material stays inside the transient crater (see, for example, refs [45–47]). In addition, these values are supported by the detection of impactor relics in the Apollo samples (see refs [69,70] for example). These impactor relics were thought to originate from ejecta from the Imbrium or Serenitatis basins.

Size–frequency distribution and impact flux for Monte Carlo models. The size-frequency distribution (SFD) of projectiles colliding with the Moon can be obtained from the impact cratering records on the lunar surface[4], as in previous studies (for example, refs [3,58]). More specifically, we convert the crater SFD on the lunar surface[3] to the projectile SFD by using crater-to-transient-crater[71,72] and transient-crater-to-projectile-size[22] scaling laws, with a prescribed distribution of impact velocities[20] and probability of impact angles[21] on the Moon. We then generate random impactors to reproduce the craters and basins as observed on the lunar surface. The number of large objects in the population can conceivably be constrained by the large basins observed on the lunar surface, provided that these impacts took place after the formation of the Moon's crust. For basins on the lunar surface, the largest confirmed impact structure is the South Pole–Aitken basin with a size of roughly 2,500 km. However, it is conceivable that the traces of some very large objects that struck the early Moon are not preserved (such as in the Procellarum megabasin, with a diameter of 3,200 km; ref. [73]), or that such events did not leave behind obvious surface or gravity expressions[74]. Our model predicts that the Moon was hit by more than one impactor forming South Pole–Aitken size structure (or larger)[66]. Although the basin record of the Moon shows only one basin of this size[30,31,73], the prediction of our model is probably not invalidated because large-scale impact structures on the early Moon may relax quickly[32] and therefore may now be invisible on the present-day surface.

Concerning the impact rate, we considered two classic scenarios. The nominal model assumes that the lunar bombardment has decayed monotonically since the time of formation of the Moon[4]. The other model is the so-called sawtooth bombardment scenario, with a discontinuous impact bombardment profile[3]. In ref. [9], a new scenario for the Moon's impact history is proposed on the basis of numerical simulations of planetesimals leftover from the period of terrestrial planet formation. The production function obtained in this new scenario is very similar to that proposed in ref. [4], but it is curved upward mostly before 4.35 Gyr ago. Therefore the result regarding the HSE retention age of the lunar crust and mantle would not change substantially, and so we do not consider the new impact scenario here. The production functions that we do consider are shown in Extended Data Fig. 4. For the nominal case, we extrapolate the curve up to 4.50 Gyr ago, similar to earlier works (for example, refs [3,58]). Both curves start at 4.50 Gyr ago, which is the most commonly assumed time of Moon formation[25].

Impactor mass accreted to the Moon. In the Monte Carlo simulation, we varied the starting time from which we calculate the mass accreted to the Moon to the present day. With the assigned impactor flux (see ref. [4] for example), we estimated the total number of impactors between the starting time and the present day. For each individual impact within a time interval, we estimated the transient crater diameter and depth according to the scaling laws derived from laboratory impact experiments[75] and numerical modelling[52]. If the depth of the transient crater (d_{tr}) is larger than the average crustal thickness, the impact is assumed to penetrate the crust and the retained impactor mass trapped within the transient cavity is thought to be transported directly into the lunar mantle, whereas the fraction of retained impactor deposited beyond the rim of the transient crater is assumed to mix with the crust. In all other cases, the total retained impactor mass is mixed with the crust. The latter assumption is reasonable because small projectiles do not penetrate the crust and therefore cannot transport the retained material to the mantle. For large objects that punch through the crust, the impact produces large volumes of impact melt[76,77], forming a melt sheet that connects to the mantle[78]. The fraction of retained impactor materials trapped within the transient cavity can be directly transported into the mantle through the impact melt pool[78,79], leaving just the fraction of retained material deposited beyond the transient cavity to mix with the crust. For simplicity, we assume in our Monte Carlo calculations that around 96% of the retained impactor material is trapped within the transient crater and transported into the mantle, and the remaining 4% or so of the retained impactor material is deposited beyond the transient crater rim and mixed with the crust (Extended Data Fig. 3). This assumption is reasonable because our results are not sensitive to the fraction of the retained impactor material mixed with the crust (see below).

We use the average crustal thicknesses of 34 km and 43 km derived from the GRAIL data[23] as a lower and upper limit for the crustal thickness of the Moon. As the crust is thought to have formed very soon after the Moon formed[24,27], we assume that the crustal thickness is constant over time in our calculation. For each starting time, we repeat the Monte Carlo procedure millions of times to address the stochastic variability intrinsic to the bombardment process, and record the masses accreted to the crust and mantle. Note that for differentiated impactors ($d > 300$ km; ref. [50]) for which the impactor's core is accreted to the Moon (Extended Data Fig. 5a), we assume that the retained material of the impactors and their (retained) HSEs are fully merged into the lunar crust and/or mantle. Although these assumptions are probably true for small impactors, larger objects (with diameters much greater than 300 km), are to some extent thought to merge a fraction of their cores with the core of the Moon directly during the impact. We analysed our impact simulations with $d = 300$–560 km, and found that none of the accreted impactor's cores merge with the core of the Moon directly. However, as the impactor core is approximately assumed as the central region of a homogenous impactor with the same material and density as the lunar mantle, rather than the denser metal material that can reach the Moon's core via impact, the fraction of the retained core merged with the Moon's core is underestimated to some extent in our simulations. Several additional impact models with $d = 640$–960 km show that only impacts with high impact angles (greater than 70°) have a small fraction of their retained core material directly merged with the Moon's core. This fraction increases with the impactor diameter and impact angle, but never exceeds around 10%. However, such large impactors are extremely rare in the Moon's impact history, and tend to have low impact angles (for example, less than 30°) in our Monte Carlo simulations; therefore, the fraction of accreted impactor core material that has directly merged with the Moon's core is considered to be insignificant. In our calculations, we record the total mass of the bodies accreted to the Moon. However, for low-angle impacts, for which the impactor's core is not accreted (Extended Data Fig. 5b), we do not record any mass (from the mantle and crust of the impactor) accreted to the Moon, because the HSE concentrations in the crust and mantle

of differentiated impactors are expected to be very low. Figure 3 shows the mass accreted into the crust and mantle for crustal thicknesses of 34 km and 43 km with the impact flux of ref. [4]. Our results indicate that the thicker lunar crust increases the proportion of materials accreted into the crust. However, the masses accreted into the crust are within the ranges inferred from the crustal HSE budget. We also did a similar calculation with the assumption that around 10% of the retained impactor is deposited beyond the transient crater and is mixed with the crust (Extended Data Fig. 6). Our results show that the masses accreted into the crust and mantle are still within the ranges inferred from the HSE budgets. Impactors accreted to the crust and mantle reach the masses inferred from the HSE concentrations if HSE retention began at around 4.35 Gyr.

HSEs are known to be removed from the mantle by metal segregation during core formation. Because the Moon's core should have formed quickly after lunar formation[25], the HSEs in the lunar mantle and crust have been used to constrain the amount of chondritic material hitting the Moon since its formation. With an average impactor-retention ratio of 0.6 (two to three times larger than the value derived from this study), the total mass accreted by the Moon exceeds that predicted from the HSE budget by almost an order of magnitude if the impact flux of ref. [4] is adopted (as in ref. [3]). As a consequence, an impact flux was designed[3] with a sawtooth-like profile (see Extended Data Fig. 4) in order to reconcile the formation of numerous craters and basins at the time of the late heavy bombardment (at times younger than 4.1 Gyr ago) with the total mass accreted to the Moon as inferred from HSEs. Although our new results indicate a lower impactor-retention ratio (roughly two to three times smaller than previously[1,3]), this does not reconcile the impact flux of ref. [4] with the lunar HSE budgets if the lunar crust and mantle have retained HSEs since the time of lunar formation (around 4.50 Gyr ago). Only if the mantle started to retain HSEs from 4.35 Gyr ago (around 150 million years after Moon formation)—as proposed in ref. [9] and here—can the lunar HSE budget be explained with the impact flux of ref. [4]. In this case, the sawtooth profile of the production function is no longer needed. The sequestration of HSEs accreted into the lunar core before 4.35 Gyr ago probably involved sulfide segregation to the lunar core during the end of LMO crystallization and mantle overturn (see ref. [9] for example).

Average impactor-retention ratio for the Earth. The Earth's escape velocity is almost five times higher than that of the Moon (11.2 km s^{-1} versus 2.4 km s^{-1}). The total mass of escaping impactor material is around 5% and 25% for impact angles of 30° and 15°, respectively, and is negligible at higher impact angles[80]. Thus, the impactor-retention ratio for the Earth is only slightly less than 1.

Data availability

The data that support the findings of this study are available from the corresponding author on request.

Code availability

At present, the iSALE code is not fully open source. It is distributed on a case-by-case basis to academic users in the impact community, strictly for non-commercial use. Scientists interested in using or developing iSALE should see http://www.isale-code.de for a description of application requirements. The Monte Carlo code used here is available from the corresponding author on request.

34. Day, J. M. D., Pearson, D. G. & Taylor, L. A. Highly siderophile element constraints on accretion and differentiation of the Earth-Moon system. *Science* **315**, 217–219 (2007).
35. Day, J. M. D., Brandon, A. D. & Walker, R. J. Highly siderophile elements in Earth, Mars, the Moon, and Asteroids. *Rev. Mineral. Geochem*. **81**, 161–238 (2016).
36. Day, J. M. D. Geochemical constraints on residual metal and sulfide in the sources of lunar mare basalts. *Am. Mineral*. **103**, 1734–1740 (2018).
37. Walker, R. J., Horan, M. F., Shearer, C. K. & Papike, J. J. Low abundances of highly siderophile elements in the lunar mantle: evidence for prolonged late accretion. *Earth Planet. Sci. Lett.* **224**, 399–413 (2004).
38. Taylor, G. J. & Wieczorek, M. A. Lunar bulk chemical composition: a post-Gravity recovery and Interior Laboratory reassessment. *Phil. Trans. A* **372**, 20130242 (2014).
39. Morgan, J. W., Gros, J., Takahashi, H. & Hertogen, H. Lunar breccia 73215: siderophile and volatile elements. *Proc. Lunar Sci. Conf*. **7**, 2189–2199 (1976).
40. Gros, J., Tahahashi, H., Hertogen, J. Morgan, J. W. & Anders, E. Composition of the projectiles that bombarded the lunar highlands. *Proc. Lunar Sci. Conf*. **7**, 2403–2425 (1976).
41. Norman, M. D., Bennett, V. C. & Ryder, G. Targeting the impactors: siderophile element signatures of lunar impact melts from Serenatatis. *Earth Planet. Sci. Lett*. **202**, 217–228 (2002).
42. Puchtel, I. S. et al. Osmium isotope and highly siderophile element systematics of lunar impact melt breccias: implications for the late accretion history of the Moon and Earth. *Geochim. Cosmochim. Acta* **72**, 3022–3042 (2008).
43. Gleißner, P. & Becker, H. Formation of Apollo 16 impactites and the composition of late accreted material: constraints from Os isotopes, highly siderophile elements and sulfur abundances. *Geochim. Cosmochim. Acta* **200**, 1–24 (2017).
44. Schultz, P. H. & Gault, D. E. Prolonged global catastrophes from oblique impacts. *Spec. Pap. Geol. Soc. Am*. **247**, 239–262 (1990).
45. Daly, R. T. & Shultz, P. H. Predictions for impactor contamination on Ceres based on hypervelocity impact experiments. *Geophys. Res. Lett*. **42**, 7890–7898 (2015).
46. Daly, R. T. & Shultz, P. H. Delivering a projectile component to the vestan regolith. *Icarus* **264**, 9–19 (2016).
47. Daly, R. T. & Schultz, P. H. Projectile preservation during oblique hypervelocity impacts. *Meteorit. Planet. Sci*. **54**, 1364–1390 (2018).
48. Thompson, S. L. & Lauson, H. S. *Improvements in the CHART D Radiation-Hydrodynamic Code III: Revised Analytic Equations of State*. Report SC-RR-71 0714 (Sandia National Laboratory, 1972).
49. Benz, W. et al. The origin of the Moon and the single-impact hypothesis III. *Icarus* **81**, 113–131 (1989).
50. Lee, D.-C. & Halliday, A. N. Core formation on Mars and differentiated asteroids. *Nature* **388**, 854–857 (1997).
51. Davison, T. M. et al. Numerical modeling of oblique hypervelocity impacts on strong ductile targets. *Meteorit. Planet. Sci*. **46**, 1510–1524 (2011).
52. Potter, R. W. et al. in *Large Meteorite Impacts and Planetary Evolution V* (eds Osinski, G. R. & Kring, D. A.) 99–113 (Lunar and Planetary Institute, 2015).
53. Marchi, S. et al. A new chronology for the Moon and Mercury. *Astron. J*. **137**, 4936–4948 (2009).
54. Collins, G. S., Melosh, H. J. & Ivanov, B. A. Modeling damage and deformation in impact simulations. *Meteorit. Planet. Sci*. **39**, 217–231 (2004).
55. Ahrens, T. J. & O'Keefe, J. D. Shock melting and vaporization of lunar rocks and minerals. *Moon* **4**, 214–249 (1972).
56. Pierazzo, E., Vickery, A. M. & Melosh, H. J. A reevaluation of impact melt product. *Icarus* **127**, 408–423 (1997).
57. Pierazzo, E. & Melosh, H. J. Hydrocode modeling of oblique impacts: the fate of the projectile. *Meteorit. Planet. Sci*. **35**, 117–130 (2000).
58. Marchi, S. et al. Widespread mixing and burial of Earth's hadean crust by asteroid impacts. *Nature* **511**, 578–582 (2014).
59. Schultz, P. H. & Sugita, S. Fate of the Chicxulub impactor. In *28th Annu. Lunar Planet. Sci. Conf*. 1261–1262 (1997).
60. Collins, G. S., Miljkovic, K. & Davison, T. M. The effect of planetary curvature on impact crater ellipticity. *EPSC Abstr.* **8**, EPSC2013-989 (2013).
61. Bottke, W. F. et al. Dating the Moon-forming impact event with asteroidal meteorites. *Science* **348**, 321–323 (2015).
62. Laneuville, M., Wieczorek, M., and Breuer, D. Asymmetric thermal evolution of the Moon. *J. Geophys. Res. Planets* **118**, 1435–1452 (2013).
63. Ivanov, B. A. & Artemieva, N. A. in *Catastrophic Events and Mass Extinctions: Impacts and Beyond* Vol. 356 (eds Koeberl, C. & MacLeod, K. G.) 619–630 (Geological Society of America, 2002).
64. Miljkovic, K. et al. Asymmetric distribution of lunar impact basins caused by variations in target properties. *Science* **342**, 724–726 (2013).
65. Freed, A. M. et al. The formation of lunar mascon basins from impact to contemporary form. *J. Geophys. Res*. **119**, 2378–2397 (2014).
66. Potter, R. W. K. et al. Constraining the size of the South Pole-Aitken basin impact. *Icarus* **220**, 730–743 (2012).
67. Zhu, M. -H. et al. Numerical modeling of the ejecta distribution and formation of the Orientale basin. *J. Geophys. Res*. **120**, 2118–2134 (2015).
68. Melosh, H. J. *Impact Cratering: A Geological Process* (Oxford Univ. Press, 1989).
69. Joy, K. H. et al. Direct detection of projectile relics from the end of the lunar basin-forming epoch. *Science* **336**, 1426–1429 (2012).
70. Liu, J. G. et al. Diverse impactors in Apollo 15 and 16 impact melt rocks: evidence from osmium isotopes and highly siderophile elements. *Geochim. Cosmochim. Acta* **155**, 122–153 (2015).
71. Croft, S. K. The scaling of complex craters. *Proc. Lunar Planet. Sci. Conf*. **16**, 828–842 (1985).
72. McKinnon, W. B. & Schenk, P. M. Ejecta blanket scaling on the Moon and Mercury and interferences for projectile populations. *Lunar Planet. Sci*. **XVI**, 544–545 (1985).
73. Wilhelms, D. E. *The Geologic History of the Moon*. USGS Professional Paper 1348 (US Geological Survey, 1987).
74. Miljkovic, K. et al. Elusive formation of impact basins on the young Moon. In *Proc. 48th Lunar Planetary Science Conference* 1361 (2017).
75. Gault, D. E. & Wedekind, J. A. Experimental studies of oblique impact. In *Proc. 9th Lunar Planetary Science Conference* 3843–3875 (1978).
76. Pierazzo, E. & Melosh, H. J. Melt production in oblique impacts. *Icarus* **145**, 252–261 (2000).
77. Pierazzo, E. & Melosh, H. J. Understanding oblique impacts from experiments, observations and modeling. *Annu. Rev. Earth Planet. Sci*. **28**, 141–167 (2000).
78. Jones, A. P. et al. Impact induced melting and the development of large igneous provinces. *Earth Planet. Sci. Lett*. **202**, 551–561 (2002).
79. Kendall, J. D. & Melosh, H. J. Differentiated planetesimals impacts into a terrestrial magma ocean: fate of the iron core. *Earth Planet. Sci. Lett*. **448**, 24–33 (2016).
80. Shuvalov, V. V. et al. Crater ejecta: markers of impact catastrophes. *Phys. Solid Earth* **48**, 241–255 (2012).

Acknowledgements We thank J. M. D. Day and R. J. Walker for useful discussions. We acknowledge the developers of iSALE (www.isale-code.de), in particular D. Elbeshausen, who developed iSALE-3D. M.-H.Z. is supported by the Science and Technology Development Fund of Macau (079/2018/A2). K.W.,

H.B., N.A. and M.-H.Z. are funded by Deutsche Forschungsgeimenschaft (DFG) grant SFB-TRR 170 (A4, C2), TRR-170 Pub. No. 55. Q.-Z.Y. is funded by the NASA Emerging Worlds Program (NNX16AD34G).

Author contributions M.-H.Z. conceived the idea and performed the impact simulations. N.A. performed the Monte Carlo modelling. M.-H.Z., A.M., Q.-Z.Y, H.B. and K.W. interpreted the results. All authors contributed to the discussion of the results and wrote the manuscript.

Competing interests The authors declare no competing interests.

Additional information
Correspondence and requests for materials should be addressed to M.-H.Z.
Peer review information *Nature* thanks James Day and the other anonymous reviewer(s) for their contribution to the peer review of this work.

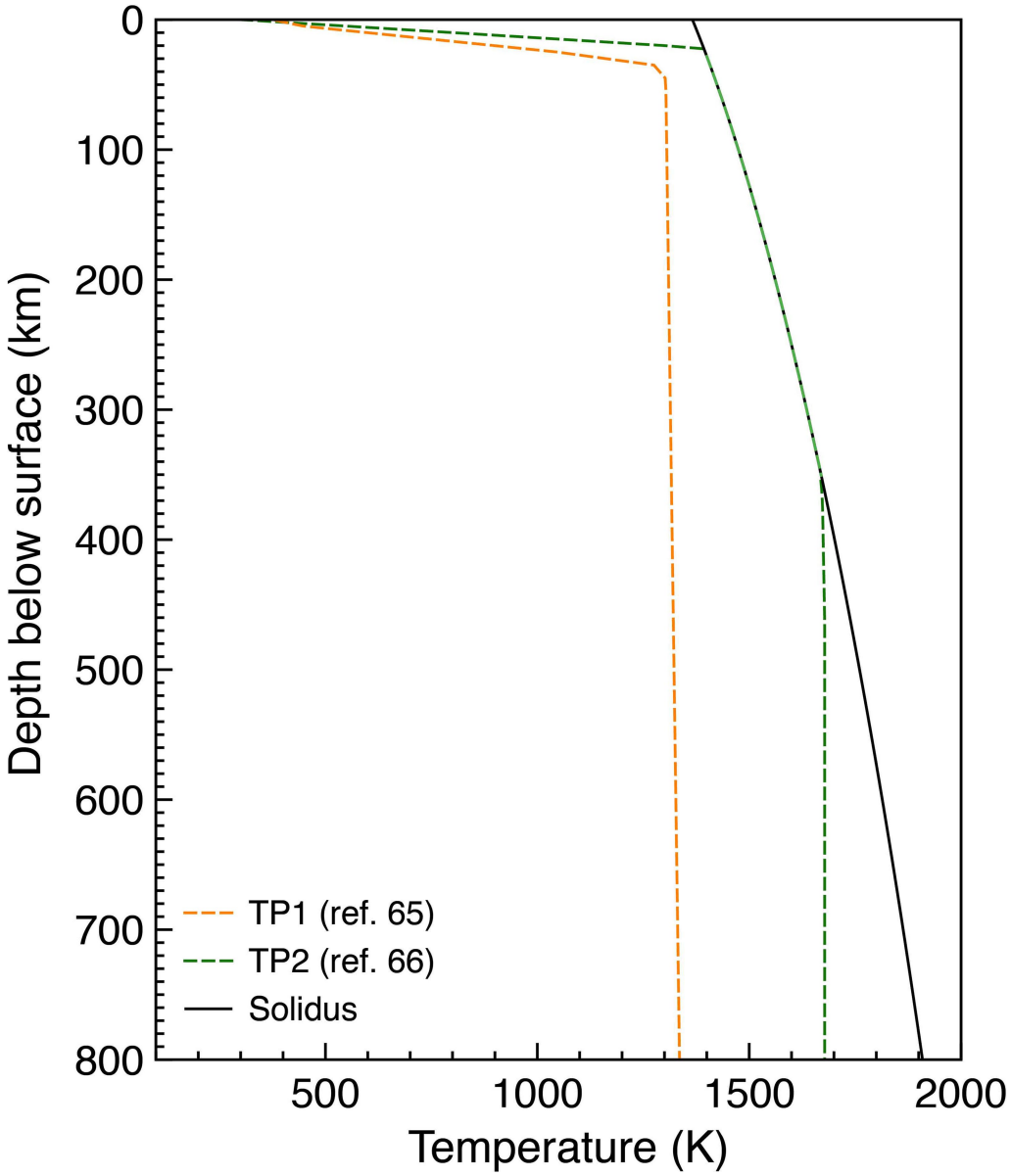

Extended Data Fig. 1 | Thermal profiles of the Moon. Two possible thermal profiles (TP1 and TP2) for the Moon, which we use in this study to test the effects of temperature on the impactor-retention ratio.

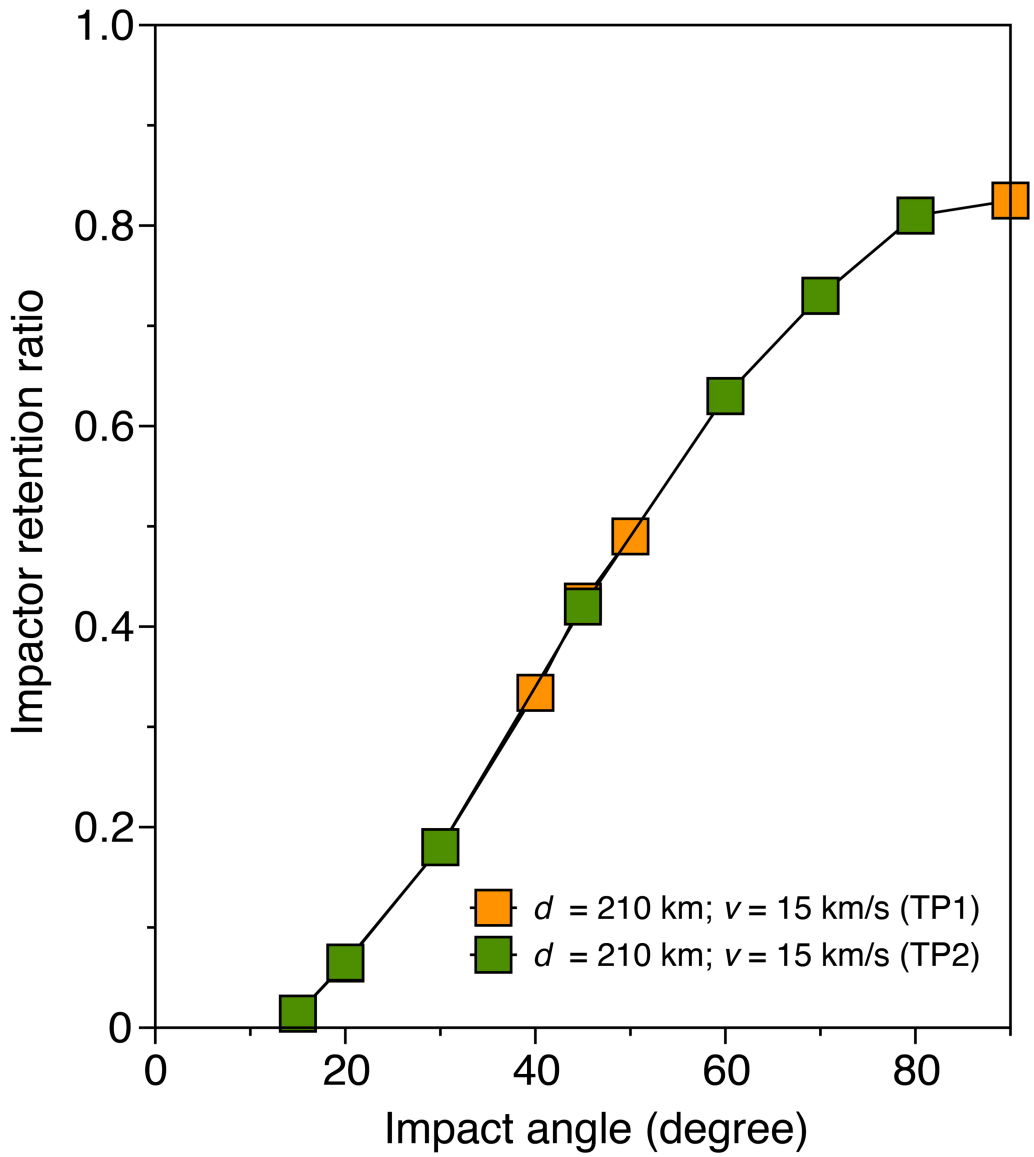

Extended Data Fig. 2 | Effects of lunar thermal profiles on the impactor-retention ratio. We calculated impactor-retention ratios for oblique impacts of impactors with diameters (d) of 210 km and velocities (v) of 15 km s^{-1}. The impact angles were varied from 15° to 90°. TP1 and TP2 represent the temperature profiles used here (Extended Data Fig. 1).

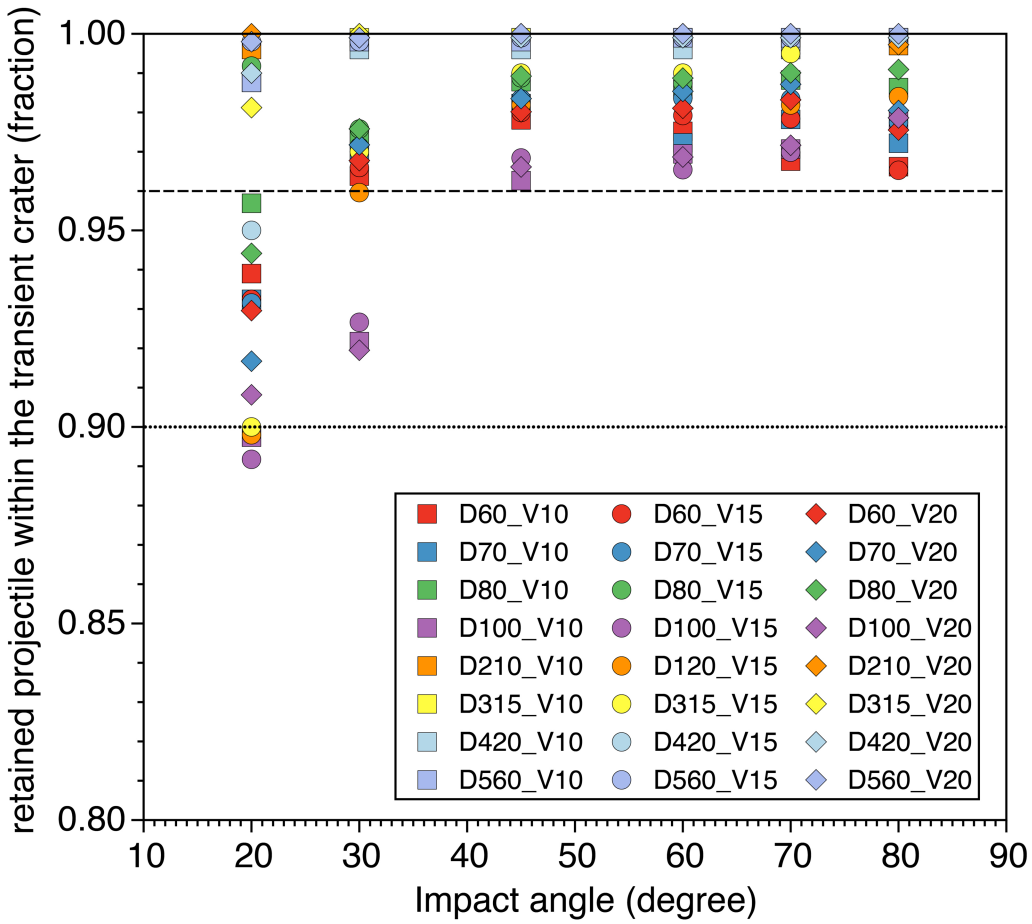

Extended Data Fig. 3 | Fraction of retained impactor material deposited within the transient crater in all simulations. In our simulations, this fraction is between 0.9 and 1.0 for impact angles greater than 20° (relative to the lunar surface). For large impactors ($d > 100$ km) with impact angles smaller than 20°, the fraction of retained material within the transient cavity is less than 0.9. The dashed line represents the fraction of 0.96 that we use in our calculations (see Fig. 3) for simplicity. The dotted line represents the fraction of 0.90 used in Extended Data Fig. 6. The numbers in the key represent the impactor diameter (D) and impact velocity (V).

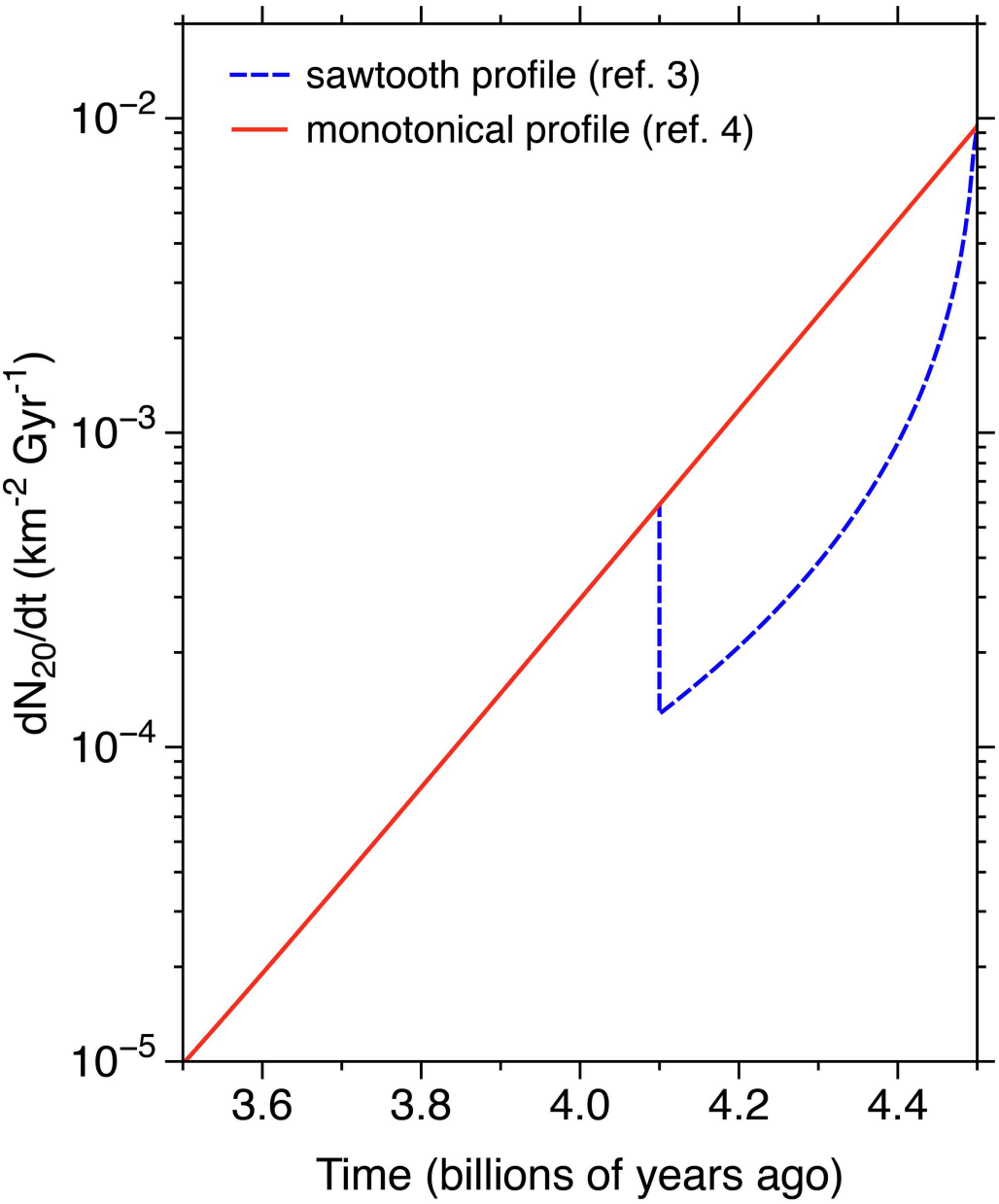

Extended Data Fig. 4 | Lunar impact fluxes. The differential number of lunar craters larger than 20 km as a function of time for the production functions discussed in the text[4,9].

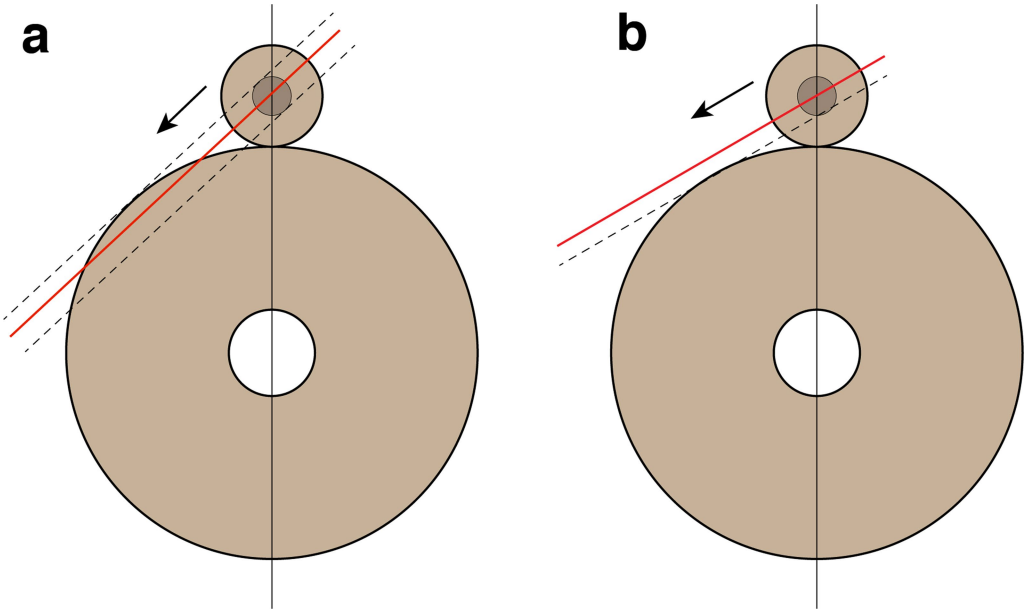

Extended Data Fig. 5 | Two scenarios involving a differentiated impactor hitting the Moon. The arrows represent the impact direction and the lines show the extent of interaction of the impactor core with the Moon. When the core of a differentiated impactor is accreted to the Moon (**a**), we record the total mass of impactors accreted to the Moon. However, when the impactor's core is not accreted to the Moon (**b**), we do not record any accreted mass. This simplification is justified because in reality the HSEs of a differentiated impactor should almost entirely be dominated by its core.

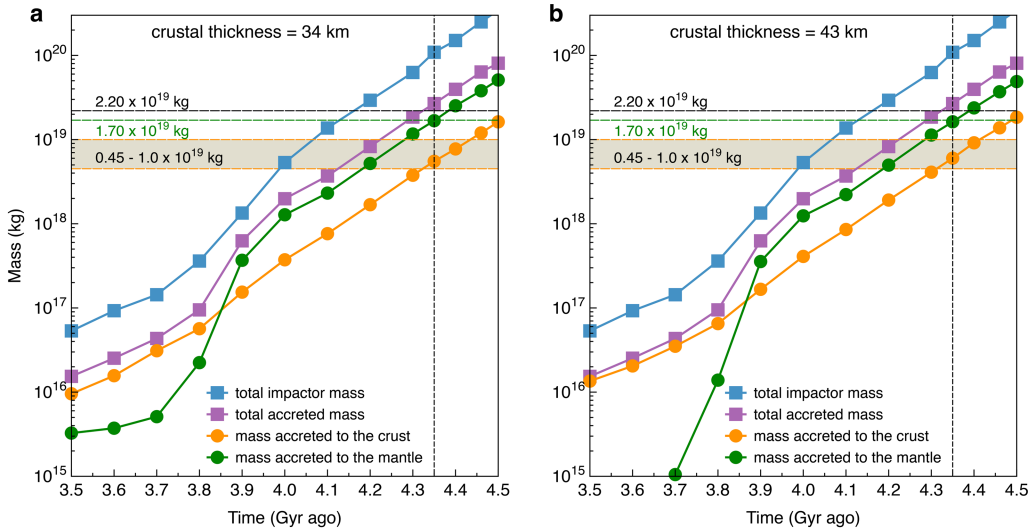

Extended Data Fig. 6 | Cumulative impactor masses that hit and are accreted into the Moon. a, **b**, The total impactor masses hitting the Moon (blue) and being accreted to the Moon (purple) from different starting times (between 4.5 Gyr to 3.5 Gyr ago) to the present day, for assumed crustal thicknesses of 34 km (**a**) and 43 km (**b**). The cumulative masses accreted to the lunar crust (orange) and mantle (green) are estimated separately. This figure is similar to Fig. 3, except that we assume that around 10% of the retained impactor material is deposited beyond the transient crater and mixed with the crust.

Extended Data Table 1 | Parameters of exponent functions for impactor-retention ratio

Impact velocity (km/s)	Impact angle (degree)	a	b
10	20	0.252	16.596
	30	0.386	10.397
	45	0.596	6.269
	60	0.688	1.114
	70	0.815	1.016
	80	0.843	0.344
15	20	0.234	20.120
	30	0.455	14.673
	45	0.671	7.049
	60	0.724	2.564
	70	0.778	0.923
	80	0.833	0.254
20	20	0.216	21.880
	30	0.432	14.255
	45	0.678	7.822
	60	0.782	2.496
	70	0.852	0.959
	80	0.883	0.397

Shown are the parameters of the fitted exponential function $f = a \times \exp(-b \times x)$ for oblique impacts (at fixed impact velocity and speed) in our simulations of the impactor-retention ratio. Here x represents the ratio of the impactor's diameter to that of the Moon. See Fig. 1.

Extended Data Table 2 | Model parameters used in iSALE-3D simulations

Model parameters	
Cells per projectile radius (CPPR)	20
Gravity (m/s^2)	1.62
Mantle thickness (km)	1,390
Core radius (km)	350
Impact velocity (km/s)	10; 15; 20
Impactor diameter (km)	10-560
Surface temperature (K)	220

Description	Mantle (target/impactor)	Core (target/impactor)
Equation of state	Dunite ANEOS*	Iron ANEOS†
Melt temperature at zero pressure (K)	1373‡	1,811§
Constant in thermal softening law	2.0‡	2.0§
Constant in Simon approximation (GPa)	1.4‡	107§
Exponent in Simon approximation	5.0‡	1.76§
Poisson's ratio	0.25	0.30§
Cohesion (damaged) (MPa)	0.01¶	-
Coefficient of internal friction for material (damaged)	0.6¶	-
Limiting strength at high pressure (damaged) (GPa)	3.5¶	-
Cohesion (intact) (MPa)	50¶	100§
Coefficient of internal friction for material (intact)	1.5¶	-
Limiting strength at high pressure (intact) (GPa)	3.5¶	-

*See ref. [49].
†See ref. [48].
‡See ref. [54].
¶See refs [52,64,66] and references therein for a description of the model strength parameters and their implementation in iSALE.
§See ref. [66] and references therein for a description of the model strength parameters and their implementation in iSALE.